

## Highlights from the NA61/SHINE

Szymon Pulawski<sup>1,\*</sup> on behalf of NA61/SHINE

<sup>1</sup>Institute of Physics, University of Silesia, Katowice, Poland

**Abstract.** NA61/SHINE is a multipurpose fixed-target facility at the CERN Super Proton Synchrotron. The main goals of the NA61/SHINE strong-interactions program are to discover the critical point of strongly interacting matter as well as to determine the properties of produced particles relevant for the study of the onset of deconfinement - the transition between the state of hadronic matter and the quark-gluon plasma. An analysis of hadron production properties is performed in nucleus-nucleus, proton-proton, and proton-nucleus interactions as a function of collision energy and size of the colliding nuclei to achieve these goals.

The selected NA61/SHINE results from this program are presented. In particular, the latest results from different reactions p+p, Be+Be, Ar+Sc, and Pb+Pb on hadron spectra and fluctuations are discussed. The NA61/SHINE results are compared with worldwide experiments and predictions from various theoretical models, like EPOS, PHSD, UrQMD, and others.

### 1 The NA61/SHINE facility

The NA61/SHINE detector [1] is a large acceptance hadron spectrometer with excellent capabilities in charged particle momentum measurements and identification by a set of eight Time Projection Chambers as well as Time-of-Flight detectors. The high resolution forward calorimeter, the Projectile Spectator Detector (PSD), measures energy flow around the beam direction, which in nucleus-nucleus reactions is primarily a measure of the number of projectile spectator (non-interacted) nucleons and is thus related to the violence (centrality) of the collision. A set of beam detectors identifies beam particles and measures precisely their trajectories. The NA61/SHINE detector system was recently upgraded: readout rate was increased to 1kHz, new Vertex Detector and data acquisition and trigger systems were installed, extension of PSD was performed. The schematic view of upgraded system is shown in Fig. 1.

### 2 Study of the onset of deconfinement

NA61/SHINE performed a two-dimensional scan in collision energy (13A-150A GeV/c and system size (p+p, Be+Be, Ar+Sc, Xe+La, Pb+Pb) to study the phase diagram of strongly interacting matter. The main goals of NA61/SHINE are the search for the critical point and a study of the onset of deconfinement.

A plateau ("step") in the energy dependence of the inverse slope parameter  $T$  was observed by the NA49 experiment in Pb+Pb collisions for  $m_T$  spectra of  $K^\pm$ . It was expected

---

\*e-mail: [s.pulawski@cern.ch](mailto:s.pulawski@cern.ch)

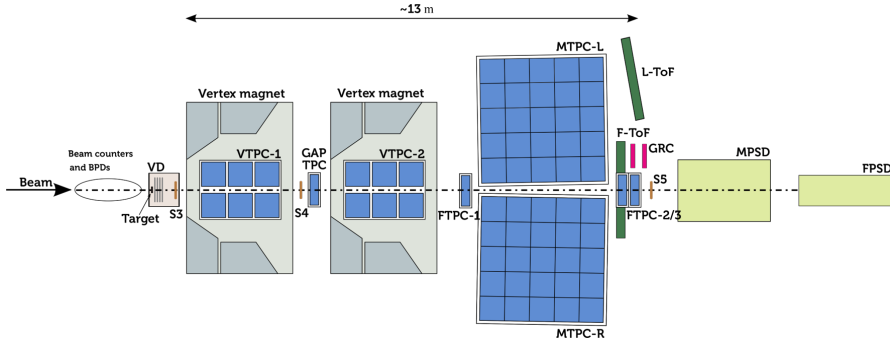


**Figure 1.** Schematic layout of NA61/SHINE detector system.

for the onset of deconfinement due to the presence of a mixed phase of hadron gas (HRG) and quark-gluon plasma (QGP) [2]. In p+p interactions at SPS energies the inverse slope parameter  $T$  of  $m_T$  spectra shows qualitatively similar energy dependence as in central Pb+Pb collisions ("step") and such a behaviour seems to emerge also in Be+Be reactions, as visible in Fig. 2. The values of the  $T$  parameter in Be+Be collisions are slightly above those in p+p interactions. The  $T$  parameter in Ar+Sc reactions is found between those in p+p/Be+Be and Pb+Pb collisions.

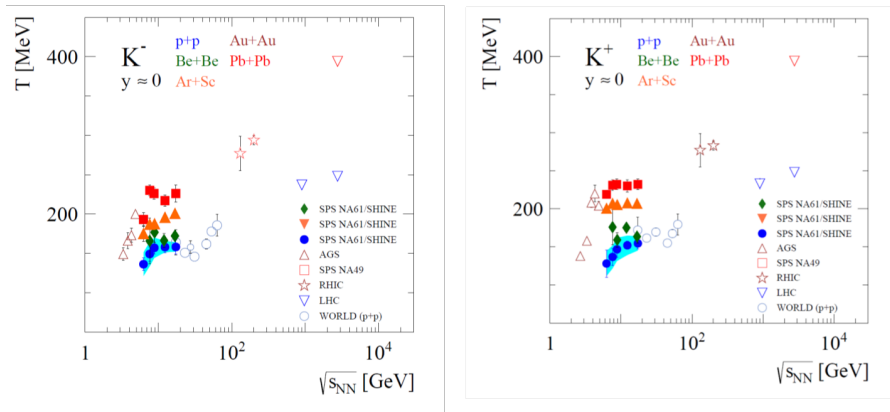


**Figure 2.** Inverse slope parameter  $T$  of  $m_T$  spectra of  $K^\pm$  as function of collision energy. Most results are shown with statistical uncertainties only. For the p+p data the shaded band indicates systematic uncertainties.

Finally, rapid changes of the ratios  $K^+/\pi^+$  at mid-rapidity and  $\langle K^+ \rangle / \langle \pi^+ \rangle$  as function of collision energy ("horn") were observed in Pb+Pb collisions by the NA49 experiment. These were predicted by the SMES model [3] as a signature of the onset of deconfinement. These two ratios together with new NA61/SHINE results from Be+Be and Ar+Sc collisions are shown in Fig. 3. A plateau like structure is visible in p+p interactions. The ratio  $K^+/\pi^+$  at mid-rapidity as well as the ratio of total yields from Be+Be collisions is close to the p+p measurements. For the five analysed energies of Ar+Sc collisions, the ratio  $K^+/\pi^+$  at mid-rapidity and  $\langle K^+ \rangle / \langle \pi^+ \rangle$  are higher than in p+p collisions but show a qualitatively similar energy dependence - no horn structure visible.

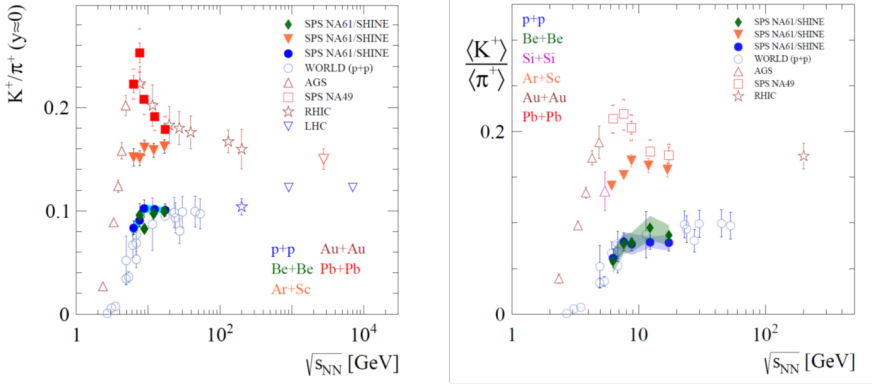


**Figure 3.** Yields ratio  $K^+/\pi^+$  at mid-rapidity and total yields ratio  $\langle K^+ \rangle / \langle \pi^+ \rangle$  produced in p+p, Be+Be and Pb+Pb collisions as function of collision energy.

The  $\Xi$  mean multiplicities measured by NA61/SHINE in inelastic  $p + p$  interactions are used to calculate the enhancement factors of  $\Xi$ s observed in centrality selected Pb+Pb, in semi-central C+C, and in Si+Si collisions as measured by NA49 [4] at the CERN SPS. The results for mid-rapidity densities are shown in Fig. 4 (*left*) as a function of  $\langle N_W \rangle$ . The enhancement factor increases approximately linearly from 3.5 in C+C to 9 in central Pb+Pb collisions. With the advent of the NA61/SHINE results on  $\Xi$  production in  $p + p$  interactions a new baseline reference becomes available and it is used here for the recalculation of the enhancement observed in the NA57  $p$ +Be and A+A data. Figure 4 (*right*) shows the rapidity densities  $dn/dy$  of  $\Xi^+$  at mid-rapidity per mean number of wounded nucleons divided by the corresponding values for inelastic  $p + p$  collisions as a function of  $\langle N_W \rangle$ . Apart from a slightly flatter rise the overall picture remains unchanged.

### 3 Search for critical point

The expected signal of a critical point (CP) is a non-monotonic dependence of various fluctuation or correlation measures in NA61/SHINE energy – system size scan. Fluctuations of conserved charges (electric, strangeness or baryon number) are of special interest [8–10]. To compare fluctuations in systems of different sizes, one should use quantities insensitive to system volume, i.e. intensive quantities. They are constructed by division of cumulants  $\kappa_i$  of the measured multiplicity distribution (up to fourth order), where  $i$  is the order of the cumulant. For second, third and fourth order cumulants intensive quantities are defined as:  $\kappa_2/\kappa_1$ ,  $\kappa_3/\kappa_2$  and  $\kappa_4/\kappa_2$ . Their reference values for no fluctuations are 0 and for independent particle production are 1. In case of net-charge, cumulant ratios are redefined to  $\kappa_2 / (\kappa_1 [h^+] - \kappa_1 [h^-])$ ,  $\kappa_3 / (\kappa_1 [h^+ - h^-])$  and  $\kappa_4 / (\kappa_2 [h^+ - h^-])$  in order to keep the same references. Figure 5 shows the system size and energy dependence of second, third and fourth order cumulant ratio of net-electric charge in p+p as well as central Be+Be and Ar+Sc interactions. So far, there is no clear difference between systems for higher order moments. More detailed studies are needed.

Another possible tool for search of CP is a proton intermittency. In the proximity of CP a local power-law fluctuations of the baryon density should appear which can be searched for by studying second factorial moments with the cell size or, equivalently, with the number of cells in space of protons at mid-rapidity [11–13]. NA61/SHINE measures  $F_2(M)$  using

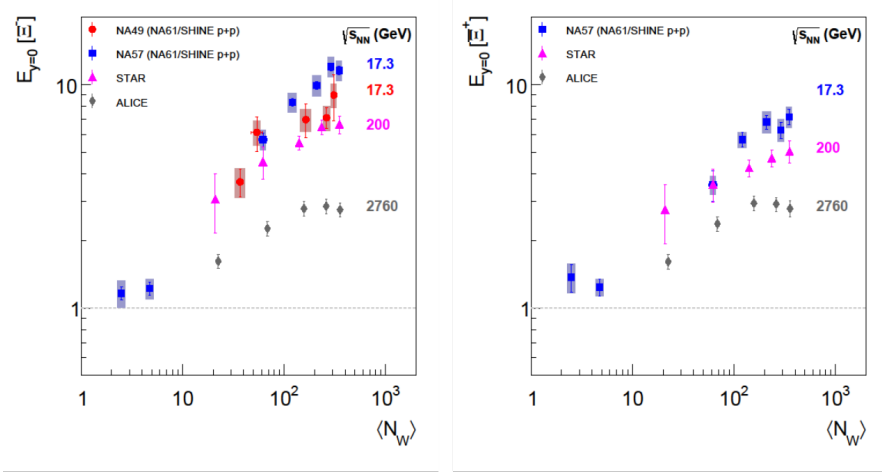


**Figure 4.** (Color online) The strangeness enhancement  $E$  at mid-rapidity as a function of average number of wounded nucleons  $\langle N_W \rangle$  calculated as a ratio of rapidity density for  $\Xi^-$  production (*left*) and  $\Xi^+$  production (*right*) in nucleus-nucleus interactions per  $\langle N_W \rangle$  divided by the corresponding value for  $p + p$  interactions. The enhancement factor is defined as  $E = \frac{2}{\langle N_W \rangle} \frac{dn/dy(A+A)}{dn/dy(p+p)}$ . At SPS energies and above the number of wounded nucleons is close to or equal to the number of participating nucleons. Red circles – NA49 Pb+Pb at 158A GeV [4], blue squares - NA57  $p$ +Be,  $p$ +Pb and Pb-Pb at the same center-of-mass energy  $\sqrt{s_{NN}} = 17.3$  GeV [5], magenta triangles - STAR Au+Au at  $\sqrt{s_{NN}} = 200$  GeV [6], gray diamonds - ALICE Pb+Pb at  $\sqrt{s_{NN}} = 2.76$  TeV [7]. The systematic errors are represented by shaded boxes.

statistically independent points and cumulative variables. Preliminary results on  $F_2(M)$  of mid-rapidity protons measured in 0-20% most central Ar+Sc collisions at 150A GeV/c and 0-10% most central Pb+Pb collisions at 30A and 13A GeV/c are presented in Fig. 6. The intermittency index  $\phi_2$  for a system freezing out at the QCD critical endpoint is expected to be  $\phi_2 = 5/6$  assuming that the latter belongs to the 3-D Ising universality class [14]. Measured  $F_2(M)$  of protons for Ar+Sc at 150A GeV/c and Pb+Pb at 30A and 13A GeV/c show no indication for power-law increase with a bin size which could indicate the presence of CP.

## 4 Strangeness production in p+p

Finally, NA61/SHINE provides new and unique results on strangeness particle production in p+p interactions. Figure 7 presents first rapidity distribution of  $K^*(892)^0$  produced in inelastic p+p interactions at 40 and 80 GeV/c [15] and the only result on  $\Xi(1530)^0$  and  $\bar{\Xi}(1530)^0$  production in inelastic p+p interactions at 158 GeV/c [16].

The new measurements by NA61/SHINE of  $\Xi(1530)^0$  and  $\bar{\Xi}(1530)^0$  produced in inelastic  $p + p$  interactions at 158 GeV/c as well as previously obtained results for  $\pi^+$ ,  $\pi^-$ ,  $K^+$ ,  $K^-$ ,  $p$ ,  $\bar{p}$ ,  $K^*(892)^0$ ,  $\Lambda$ ,  $\phi(1020)$ ,  $\Xi^-$  and  $\bar{\Xi}^+$  (see Refs. [17–23]) were fitted by different variants of the Hadron Resonance Gas Model (HRG). The Canonical Ensemble with fixed  $\gamma_s = 1$  and Canonical Ensemble with fitted strangeness saturation parameter  $\gamma_s$  configurations were used. Figure 8 compares the measured multiplicities of particles produced in inelastic  $p + p$  interactions at 158 GeV/c with multiplicities of the same particles obtained from the HRG model in the CE formulation under two different model assumptions:  $\gamma_s = 1$  and fitted  $\gamma_s$ . The

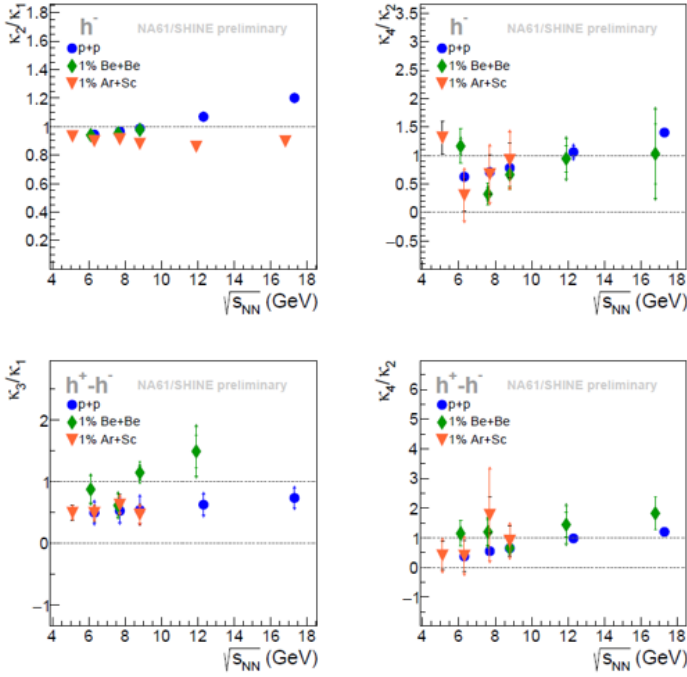


**Figure 5.** System size and energy dependence of  $\kappa_2/\kappa_1$ ,  $\kappa_4/\kappa_2$ ,  $\kappa_3/(\kappa_1 [h^+ - h^-])$  and  $\kappa_4/(\kappa_2 [h^+ - h^-])$ . Statistical uncertainty was obtained with the bootstrap method and it is indicated as a dashed black bar. Systematic uncertainty/bias: p+p - corrected data with estimate on systematic uncertainty; Be+Be/Ar+Sc - uncorrected data with estimate of systematic bias. Systematic uncertainty/bias is indicated with arrows.

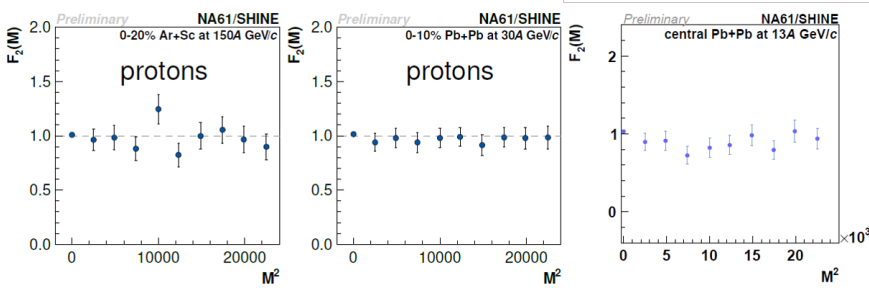


**Figure 6.** Preliminary results on  $F_2(M)$  of mid-rapidity protons measured in 0-20% most central Ar+Sc collisions at 150A GeV/c and 0-10% most central Pb+Pb collisions at 30A and 13A GeV/c.

software package THERMAL-FIST 1.3 [24] was used for this purpose. For the small  $p + p$  system, the appropriate statistical system is the Canonical Ensemble, which has as parameters the temperature  $T$ , the radius  $R$  of the system at chemical freezeout, and the strangeness suppression factor  $\gamma_s$ . The results plotted in Fig. 8 show significant discrepancies for the fitted parameters  $T$  and  $R$  between the fits with  $\gamma_s = 1$  and free  $\gamma_s$ . Moreover, the fit with

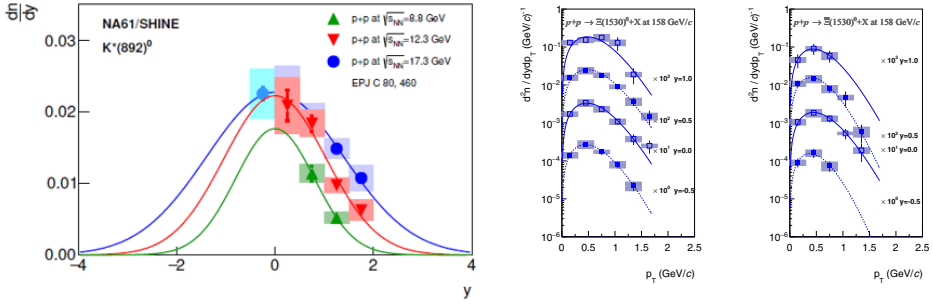


**Figure 7.** Rapidity distribution of  $K^*(892)^0$  produced in inelastic  $p+p$  interactions at 40 and 80 GeV/c and transverse momentum spectra in rapidity intervals of  $\Xi(1530)^0$  and  $\bar{\Xi}(1530)^0$  production in inelastic  $p+p$  interactions at 158 GeV/c

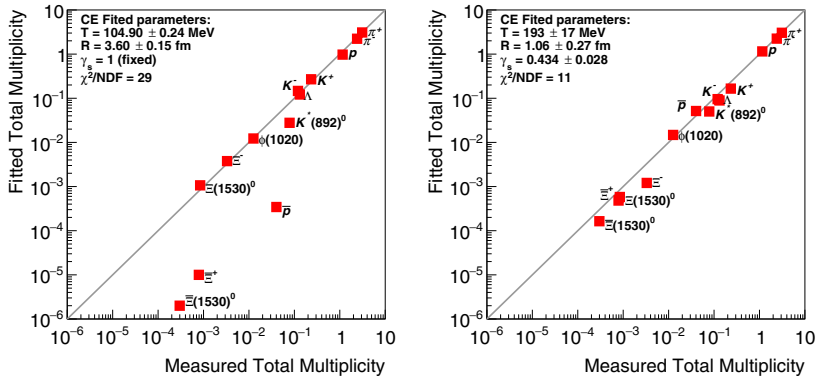


**Figure 8.** (Color online) Mean multiplicities of  $\pi^+$ ,  $\pi^-$ ,  $K^+$ ,  $K^-$ ,  $p$ ,  $\bar{p}$ ,  $K^*(892)^0$ ,  $\Lambda$ ,  $\phi(1020)$ ,  $\Xi^-$ ,  $\bar{\Xi}^+$ ,  $\Xi(1530)^0$  and  $\bar{\Xi}(1530)^0$  produced in  $p+p$  interactions at 158 GeV/c [17–23] measured by NA61/SHINE are compared with mean multiplicities obtained from the HRG model based on the Canonical Ensemble with fixed  $\gamma_s = 1$  (i) and fitted  $\gamma_s$  (ii). Uncertainties of the measurement are smaller than the symbol size.

fixed  $\gamma_s$  shows unacceptably large  $\chi^2/\text{NDF} = 29$ . This demonstrates that the statistical model fails when fixing  $\gamma_s$  to one. The fit with free  $\gamma_s$  finds  $\gamma_s = 0.434 \pm 0.028$  and reproduces the measurements significantly better than with  $\gamma_s = 1$ . Thus the statistical model indicates a strong suppression of strange particle production in  $p + p$  collisions at CERN SPS energies.

## Acknowledgment

This work was supported by the Polish Minister of Education and Science (contract No. 2021/WK/10), the Norwegian Financial Mechanism 2014-2021 (grant 2019/34/H/ST2/00585), National Science Center, Poland Grant No. 2018/31/G/ST2/03910 - BEETHOVEN CLASSIC 3 and under the Research Excellence Initiative of the University of Silesia in Katowice.

## References

- [1] N. Abgrall et al. (NA61/SHINE), JINST **9**, P06005 (2014), 1401.4699
- [2] R. Poberezhnyuk, M. Gazdzicki, M. Gorenstein (2015), 1502.05650
- [3] M. Gazdzicki, M.I. Gorenstein, Acta Phys.Polon. **B30**, 2705 (1999), hep-ph/9803462
- [4] T. Anticic et al. (NA49), Phys. Rev. C **80**, 034906 (2009), 0906.0469
- [5] F. Antinori et al. (NA57), J. Phys. G **32**, 427 (2006), nuc1-ex/0601021
- [6] B. Abelev et al. (STAR), Phys. Rev. C **77**, 044908 (2008), 0705.2511
- [7] B.B. Abelev et al. (ALICE), Phys. Lett. B **728**, 216 (2014), [Erratum: Phys.Lett.B 734, 409–410 (2014)], 1307.5543
- [8] M.A. Stephanov, Phys. Rev. Lett. **102**, 032301 (2009), 0809.3450
- [9] M. Asakawa, M. Kitazawa, Prog. Part. Nucl. Phys. **90**, 299 (2016), 1512.05038
- [10] M.A. Stephanov, K. Rajagopal, E.V. Shuryak, Phys. Rev. Lett. **81**, 4816 (1998), hep-ph/9806219
- [11] A. Bialas, R.B. Peschanski, Nucl. Phys. B **273**, 703 (1986)
- [12] L. Turko, Phys. Lett. B **227**, 149 (1989)
- [13] F.K. Diakonou, N.G. Antoniou, G. Mavromanolakis, PoS CPOD2006, 010 (2006)
- [14] H. Satz, Nucl.Phys. **B326**, 613 (1989)
- [15] A. Acharya et al. (NA61/SHINE), Eur. Phys. J. C **82**, 322 (2022), 2112.09506
- [16] A. Acharya et al. (NA61/SHINE), Eur. Phys. J. C **81**, 911 (2021), 2105.09144
- [17] N. Abgrall et al. (NA61/SHINE), Eur.Phys.J. **C74**, 2794 (2014), 1310.2417
- [18] A. Aduszkiewicz et al. (NA61/SHINE), Eur. Phys. J. **C77**, 671 (2017), 1705.02467
- [19] A. Aduszkiewicz et al. (NA61/SHINE), Phys. Rev. C **102**, 011901 (2020), 1912.10871
- [20] A. Aduszkiewicz et al. (NA61/SHINE), Eur. Phys. J. C **80**, 460 (2020), 2001.05370
- [21] A. Aduszkiewicz et al. (NA61/SHINE), Eur. Phys. J. C **80**, 199 (2020), 1908.04601
- [22] A. Aduszkiewicz et al. (NA61/SHINE), Eur. Phys. J. **C76**, 198 (2016), 1510.03720
- [23] A. Aduszkiewicz et al. (NA61/SHINE), Eur. Phys. J. C **80**, 833 (2020), 2006.02062
- [24] V. Vovchenko, H. Stoecker, Comput. Phys. Commun. **244**, 295 (2019), 1901.05249